Insertion Loss of Magnetostatic-Surface Wave Transducers—Transmission-Line Model and Experiment

Manuel J. Freire, Ricardo Marqués, *Member, IEEE,* and Francisco Medina, *Senior Member, IEEE*

***Abstract*—In this paper, a transmission-line model is developed for the computation of the insertion loss of magnetostatic-surface wave transducers and measurements are carried out by the authors to check this model. In a first step of the analysis, closed-form expressions for the solution of the telegrapher's equations for the two microstrip transducers are obtained. The insertion loss is then derived from this solution as a function of three transmission-line parameters, i.e., the propagation constant and the characteristic impedance of the YIG-loaded microstrip line and the mutual inductance between the two microstrips, these quantities being, in general, complex. In a second step, these transmission-line parameters are numerically computed by applying a full-wave method-of-moments technique. Thus, the theoretical results obtained are found to be in good agreement with experimental results.**

***Index Terms*—Leakage, magnetostatic-surface waves (MSSWs), transmission-line parameters.**

I. Introduction

THE theoretical and experimental study of the excitation of magnetostatic-surface waves (MSSWs) by microstrip transducers was reported many years ago in [1] and [2]. In these papers, the input resistance and input reactance of MSSW transducers are analyzed. The radiation resistance is computed by assuming that the surface current density on the strip is uniform across the strip width (transverse direction in the microstrip). The input resistance is then obtained from the radiation resistance by assuming that the fields are uniform along the width of the yittrium–iron–garnet (YIG) film (longitudinal direction in the microstrip). This latter assumption is taken into account in the calculation by imposing that $\beta l \ll 1$ and $\alpha l \ll 1$; β and α being, respectively, the phase and attenuation constants of the electromagnetic mode propagating along the YIG-loaded microstrip and l being the width of the YIG film. Later in the literature, several studies have presented a more realistic analysis of the excitation of MSSW by microstrip transducers by disregarding some of the restrictive hypothesis assumed in [1] and [2]. For example, in [3] and [4], the radiation resistance is calculated by allowing the current distribution to be nonuniform across the strip width. In [5], the nonuniform nature of the fields due to the finite width of the YIG film is included in the analysis, but only the delay time is calculated. Actually, the hypothesis $\beta l \ll 1$ and $\alpha l \ll 1$ can be very hardly justified, except for very short transducers, as is shown in [6]–[8].

The calculation of the transmission coefficient (or insertion loss) is one of the main goals of the theoretical analysis in the design of MSSW devices such as filters or delay lines [9], [10]. Some works have dealt with the calculation of the insertion loss of MSSW transducers [11]–[13]. In [11] and [12], the hypothesis $\beta l \ll 1$ and $\alpha l \ll 1$ is assumed. In [13], the nonuniform nature of the fields along the width of the YIG film is taken into account in the analysis by means of a superposition of modes [5]. A nonuniform current distribution is also imposed in [13] and the insertion loss is computed by numerically integrating the Poynting vector in an infinite domain. In this paper, the authors show a method for the computation of the insertion loss of MSSW microstrip transducers that takes into account the nonuniform nature of both the current distribution across the strip and the fields along the width of the YIG film using a relatively simple model. The method is based on the analysis of the currents excited in the microstrips. These currents are computed numerically by integrating in a finite domain, i.e., the strip width. Unlike in [13], no explicit computation of the Poynting vector and its numerical integration in an infinite domain are required. The method has two parts. In the first part, a transmission-line model is put forward for the microstrip transducers and the subsequent telegrapher's equations are solved analytically. A closed-form solution is obtained for the telegrapher's equations and the insertion loss is then derived from this solution as a function of both the width of the YIG film and some transmission-line parameters, i.e., the complex propagation constant and complex characteristic impedance of the YIG-loaded microstrip line, as well as the mutual inductance between the two microstrips. In the second part, these transmission-line parameters are numerically computed by applying a full-wave method-of-moments (MoM) technique. Note that, although a transmission-line model is used, the results do not correspond to that of a quasi-TEM approach since the parameters of this model are obtained following a full-wave analysis. Thus, the method accounts for MSSW transducers without restrictions on the transverse dimensions of the input and output microstrips. In addition, since the analysis does not assume that $\beta l \ll 1$ or $\alpha l \ll 1$, no restriction on the width of the YIG film is imposed. A computer code following this method has been implemented for the computation of the insertion loss of MSSW microstrip transducers with

Manuscript received February 13, 2003; revised April 11, 2003. This work was supported by the Spanish Comisión Interministerial de Ciencia y Tecnología and the European Union Feder funds under Project TIC2001-3163 and by Junta de Andalucia, Spain.

The authors are with the Microwave Group, Department of Electronics and Electromagnetism, University of Seville, 41012 Seville, Spain.

Digital Object Identifier 10.1109/TMTT.2003.817440

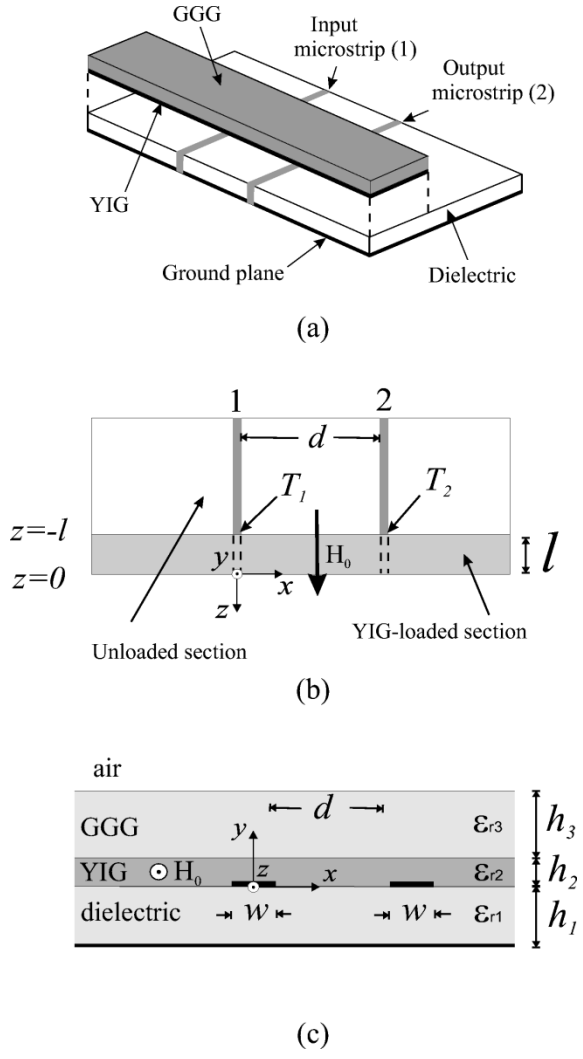

Fig. 1. (a) General view of the transducer. (b) Top view. (c) Front view.

a ground plane–dielectric–YIG–gadolinium–gallium–garnet (GGG) configuration. MSSW microstrip transducers built on different types of dielectric substrates have been measured and a good agreement has been found between the experimental and theoretical results.

II. Analysis

The geometry of the MSSW microstrip transducers analyzed in this study is shown in Fig. 1(a)–(c). In this figure, two microstrips are placed parallel at a distance d between them. The input microstrip is labeled as microstrip 1 and the output microstrip as microstrip 2. Both microstrips 1 and 2 are shorted at the end [$z = 0$ in Fig. 1(b)] and have YIG-loaded sections of length l. The first step in our method is the theoretical analysis of the telegrapher's equations in both microstrips. The telegrapher's equations are analytically solved to obtain closed-form expressions for the current distributions on both microstrips. This provides a closed-form expression for the transmission coefficient of the transducer depending on transmission-line parameters. In a second step, these transmission-line parameters are numerically calculated by means of the MoM.

A. Telegrapher's Equations

In general, the transmission coefficient S_{21} in decibels for the transducer is defined as

$$S_{21}(\mathrm{dB}) = 10\log\left(\frac{P_2}{P_1}\right). \tag{1}$$

P_1 being the injected power in the unloaded section of microstrip 1 (i.e., the part of the microstrip without YIG film) and P_2 being the power delivered to the unloaded section of microstrip 2. The expression in (1) can be written as

$$S_{21}(\mathrm{dB}) = 10\log\left(\left(1-|\Gamma|^2\right)\frac{P_2}{P_1'}\right). \tag{2}$$

P_1' being the power injected in the YIG-loaded section of microstrip 1 and Γ being the reflection coefficient at the transition between the YIG-loaded section and the unloaded section of the microstrip 1 [point T_1 in Fig. 1(b)], which is defined as

$$\Gamma = \frac{Z_{\mathrm{in}} - Z_0}{Z_{\mathrm{in}} + Z_0} \tag{3}$$

where Z_{in} is the input impedance at T_1 and Z_0 is the complex characteristic impedance of the YIG-loaded microstrip. P_1' can be written in the following form:

$$P_1' = \frac{1}{2}\mathrm{Re}(Z_{\mathrm{in}})\left|I_1(-l)\right|^2 \tag{4}$$

where $I_1(-l)$ is the amplitude of the current at T_1. Assuming that the output port (microstrip 2) is matched, P_2 can be written as

$$P_2 = \frac{1}{2}\mathrm{Re}(Z)\left|I_2(-l)\right|^2 \tag{5}$$

where Z is the characteristic impedance of the unloaded microstrip (50 Ω in the experiments carried out in this paper) and $I_2(-l)$ is the amplitude of the current at the input of the YIG-loaded section of microstrip 2 [point T_2 in Fig. 1(b)].

The currents $I_1(-l)$ and $I_2(-l)$ are obtained theoretically in this study by solving the telegrapher's equations after assuming that only one of the two microstrips is under the influence of the MSSW radiation coming from the other microstrip. This is a reasonable hypothesis since the microstrip excitation of MSSW radiation is essentially unidirectional [1]. In the geometry of Fig. 1(a)–(c), the dc magnetic bias field is directed along the z-direction so that microstrip 2 is under the influence of the radiation coming from microstrip 1. Since, in this approximation, microstrip 1 is not influenced by the presence of microstrip 2, $I_1(-l)$ is just the current at the input of a shorted transmission line of length l, i.e.,

$$I_1(-l) = I_0\cos(\gamma l). \tag{6}$$

γ being the complex propagation constant of the electromagnetic mode excited in the YIG-loaded section of the microstrip and I_0 being the complex amplitude of the current associated with this mode. The influence on microstrip 2 of the MSSW radiation coming from microstrip 1 is taken into account by assuming that the magnetic flux on the microstrip 2 is due to both

currents on microstrips 1, $I_1(z)$, and 2, $I_2(z)$. Thus, the inhomogeneous telegrapher's equations for the voltage $V_2(z)$ and the current $I_2(z)$ on microstrip 2 can be written in the following form:

$$-\frac{\partial V_2(z)}{\partial z} = j\omega M I_1(z) + j\omega L I_2(z) \tag{7}$$

$$-\frac{\partial I_2(z)}{\partial z} = j\omega C V_2(z) \tag{8}$$

where L and C are the per unit length (p.u.l.) inductance and capacitance, respectively, of the YIG-loaded microstrip and M is the p.u.l. mutual inductance between microstrips 1 and 2 through the MSSW radiation. From these equations, the following wave equation for $I_2(z)$ is derived:

$$\begin{aligned}\frac{\partial^2 I_2(z)}{\partial z^2} &= -\gamma^2 I_2(z) - \omega^2 M C I_1(z) \\ &= -\gamma^2 I_2(z) - \omega^2 M C I_0 \cos(\gamma z).\end{aligned} \tag{9}$$

The general solution of this equation is given by the sum of a particular solution $I_p(z)$ and an homogeneous solution $I_h(z)$, i.e.,

$$I_2(z) = I_p(z) + I_h(z) \tag{10}$$

$$I_p(z) = -\omega^2 M C I_0 \frac{z\sin(\gamma z)}{2\gamma} \tag{11}$$

$$I_h(z) = A\cos(\gamma z) \tag{12}$$

where A is an unknown constant. A is determined by imposing that at $z = -l$

$$V_2(-l) = -Z I_2(-l). \tag{13}$$

Once the constant A is determined, $I_2(-l)$ is obtained as

$$I_2(-l) = I_0 \frac{\omega^2 M C}{2j\gamma}\left(\frac{\gamma l + \sin(\gamma l)\cos(\gamma l)}{j\gamma\sin(\gamma l) + \omega C Z\cos(\gamma l)}\right). \tag{14}$$

After substituting (4)–(6) and (14) into (2) and taking into account that $C = \gamma/(\omega Z_0)$, an expression for S_{21} is obtained that only depends on γ, Z_0, and M [Z_{in} is computed from γ and Z_0 as in a shorted transmission line, i.e., $Z_{\text{in}} = jZ_0\tan(\gamma l)$]. This expression for S_{21} is as follows:

$$\begin{aligned}S_{21}(\text{dB}) &= 10\log\left\{\left(1 - \left|\frac{jZ_0\tan(\gamma l) - Z_0}{jZ_0\tan(\gamma l) + Z_0}\right|^2\right)\frac{Z}{\text{Re}\left(jZ_0\tan(\gamma l)\right)}\right. \\ &\quad \left.\cdot\left|\left(\frac{\omega^2 MC}{2j\gamma}\right)\frac{\dfrac{\gamma l}{\cos^2(\gamma l)} + \tan(\gamma l)}{j\gamma\tan(\gamma l) + \omega C Z}\right|^2\right\}.\end{aligned} \tag{15}$$

The computation of γ and Z_0 in this paper follows the method described by the authors of this study in a previous paper [8]. The computation of M is one of the original contributions of this paper and is carried out by using a geometry that is simpler (from the point-of-view of the analysis) than shown in Fig. 1(a)–(c). This new geometry is shown in Fig. 2 and consists of two infinite parallel YIG-loaded microstrips placed at the same distance d as in the transducer of Fig. 1(a)–(c).

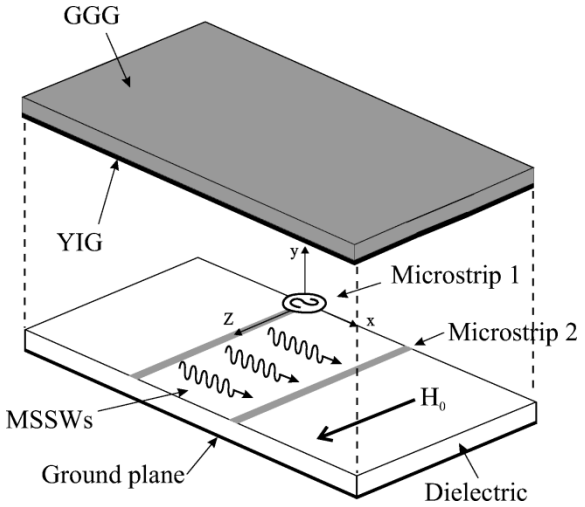

Fig. 2. Two infinite parallel YIG-loaded microstrips placed at the same distance d as in the transducer of Fig. 1(a)–(c).

The infinite microstrip 1 is fed by a delta-gap voltage source applied at the middle point $(z = 0)$. This source excites a current $I_1^{\infty}(z)$ in microstrip 1 that can be written as $(z > 0)$

$$I_1^{\infty}(z) = I_1^{\infty}\exp(-j\gamma z). \tag{16}$$

γ being the complex propagation constant of the electromagnetic mode excited in the microstrip and I_1^{∞} being the complex amplitude of the current associated with this mode (the superscript ∞ refers to the infinite length of the microstrip). Since the influence of microstrip 2 on microstrip 1 is neglected, the value of I_1^{∞} can be computed as explained in [8]. In [8], it is also shown how the complex characteristic impedance Z_0 can be directly obtained from the value of I_1^{∞}. The telegrapher's equations (7) and (8) are valid for the infinite microstrip 2 in Fig. 2. After replacing $I_1(z)$ in (7) by $I_1^{\infty}(z)$, as given in (16), the following wave equation for the current $I_2^{\infty}(z)$ in the infinite microstrip 2 is obtained:

$$\frac{\partial^2 I_2^{\infty}(z)}{\partial z^2} = -\gamma^2 I_2^{\infty}(z) - \omega^2 M C I_1^{\infty}\exp(-j\gamma z). \tag{17}$$

The general solution of this equation is given by the sum of a particular solution $I_p^{\infty}(z)$ and an homogeneous solution $I_h^{\infty}(z)$, i.e.,

$$\begin{aligned}I_2^{\infty}(z) &= I_p^{\infty}(z) + I_h^{\infty}(z) \\ I_p^{\infty}(z) &= -j\omega^2 M C I_1^{\infty}\frac{z\exp(-j\gamma z)}{2\gamma}. \\ I_h^{\infty}(z) &= B\exp(-j\gamma z).\end{aligned} \tag{18}$$

B being an unknown constant. For our analysis, it is convenient to obtain the Fourier transform of the solution (18), i.e.,

$$\widetilde{I}_2^{\infty}(k_z) = \frac{j\omega^2 M C I_1^{\infty}}{2\gamma}\frac{1}{(k_z-\gamma)^2} + jB\frac{1}{k_z-\gamma}. \tag{19}$$

Equation (19) can be written as

$$M\frac{1}{(k_z-\gamma)} = \frac{2\gamma}{j\omega^2 C I_1^{\infty}}(k_z-\gamma)\widetilde{I}_2^{\infty}(k_z) - \frac{2\gamma B}{\omega^2 C I_1^{\infty}}. \tag{20}$$

Integrating in the complex k_z-plane around $k_z = \gamma$ in (20), the second term in the right-hand side of the equation containing

B vanishes and taking into account Cauchy's theorem, M is obtained as follows:

$$M = -\frac{\gamma}{\omega^2 C\pi I_1^{\infty}} \oint (k_z - \gamma)\widetilde{I}_2^{\infty}(k_z)dk_z. \tag{21}$$

In Section II-B, the MoM is applied to compute numerically both I_1^{∞} and $\widetilde{I}_2^{\infty}(k_z)$. Once I_1^{∞} and $\widetilde{I}_2^{\infty}(k_z)$ have been obtained, the integral in (21) can be evaluated numerically to obtain M.

B. MoM

To obtain I_1^{∞} and $\widetilde{I}_2^{\infty}(k_z)$, two electric field integral equations (EFIEs) must be solved. First, I_1^{∞} is obtained by solving an EFIE for the surface current density on microstrip 1, $\mathbf{J}_1$ [8], as follows:

$$\mathbf{E}^{\text{gap}}(x,z) = \int\int_{\text{strip}} \overline{\mathbf{G}}(x,z,x',z') \cdot \mathbf{J}_1(x',z')dx'dz' \tag{22}$$

where $\mathbf{E}^{\text{gap}}(x,z)$ is the electric field imposed by the delta-gap voltage source on microstrip 1 and $\overline{\mathbf{G}}(x,z,x',z')$ is the spatial dyadic Green's function, with the variables x, x' extended from $-w/2$ to $w/2$ (w stands for the strip width) and z, z' from $-\infty$ to ∞. This EFIE is solved following the method reported in [8], which provides both the complex propagation constant and complex amplitude of the current of the mode excited in a YIG-loaded infinite microstrip fed by a delta-gap voltage source, i.e., γ and I_1^{∞}, respectively. Next, to obtain $\widetilde{I}_2^{\infty}(k_z)$, the following EFIE for the surface current density on microstrip 2, $\mathbf{J}_2$, must be solved:

$$\begin{aligned}
\mathbf{E}_{1\to 2}(x,z) + \mathbf{E}_{2\to 2}(x,z) &= 0 \qquad (23)\\
\mathbf{E}_{1\to 2}(x,z) &= \int\int_{\text{strip 1}} \overline{\mathbf{G}}(x,z,x',z') \cdot \mathbf{J}_1(x',z')dx'dz'\\
\mathbf{E}_{2\to 2}(x,z) &= \int\int_{\text{strip 2}} \overline{\mathbf{G}}(x,z,x'',z'') \cdot \mathbf{J}_2(x'',z'')dx''dz''
\end{aligned}$$

where $\mathbf{E}_{1\to 2}$ is the electric field on microstrip 2 due to the surface current density $\mathbf{J}_1$, and $\mathbf{E}_{2\to 2}(x,z)$ is the electric field on microstrip 2 due to its own surface current density $\mathbf{J}_2$. The EFIEs in (22) and (23) are solved using the Galerkin method by expanding both the transverse and longitudinal components of the surface current density $J_{i,x}$ and $J_{i,z}$ $(i = 1,2)$ into a general set of complete domain basis functions as follows:

$$\mathbf{J}_i(x,z) = J_{i,x}(x,z)\hat{\mathbf{x}} + J_{i,z}(x,z)\hat{\mathbf{z}} \tag{24}$$

$$J_{i,\alpha}(x,z) = \sum_{n=0}^{N} F_{i,\alpha,n}(x) I_{i,\alpha,n}(z), \qquad \alpha = x,z. \tag{25}$$

The $I_{i,\alpha,n}(z)$ functions are the unknown coefficients in the Galerkin problem and the $F_{i,\alpha,n}(x)$ functions are the basis functions, which are the same as in [8], i.e., both odd and even Chebyshev polynomials weighed by the proper edge condition. As in [8], these basis functions are normalized in such a way that the current on the strip is given by the coefficient related to the zeroth-order basis function, i.e., $I_i^{\infty}(z) = I_{i,z,0}(z)$. Using the guidelines of the method reported in [8], the EFIEs in (22) and (23) are transformed into the Fourier domain and, after applying the Galerkin method, a matrix equation is obtained for the Fourier transform of the unknown coefficients $\widetilde{I}_{i,\alpha,n}(k_z)$ as follows:

$$\begin{aligned}
&\sum_{\alpha,n} \Gamma_{i,(\beta,m),(\alpha,n)}(k_z) \cdot \widetilde{I}_{i,\alpha,n}(k_z)\\
&\quad = b_{i,m}(k_z), \quad i = 1,2; \quad \alpha = x,z;\ \beta = x,z;\\
&\quad m,n = 0,1,\ldots,N.
\end{aligned} \tag{26}$$

The matrix elements $\Gamma_{i,(\beta,m),(\alpha,n)}(k_z)$ are given by

$$\begin{aligned}
\Gamma_{i,(\beta,m),(\alpha,n)}(k_z) = \frac{1}{2\pi}\int_{C_{k_x}} dk_x \left[\widetilde{F}_{i,\beta,m}(k_x^*)\right]^*\\
\cdot \widetilde{G}_{\beta\alpha}(k_x,k_z)\widetilde{F}_{i,\alpha,n}(k_x)
\end{aligned} \tag{27}$$

where $\widetilde{F}_{i,\beta,m}(k_x)$ and $\widetilde{F}_{i,\alpha,n}(k_x)$ are the Fourier transforms of the basis functions in (25), $\widetilde{G}_{\beta\alpha}(k_x,k_z)$ is the $\beta\alpha$-component of the spectral dyadic Green's function (SDGF), and C_{k_x} is a proper integration path in the complex k_x-plane [8]. It must be noted that the basis functions $\widetilde{F}_{i,\beta,m}(k_x)$ and $\widetilde{F}_{i,\alpha,n}(k_x)$ are related as

$$\widetilde{F}_{2,\beta,m}(k_x) = \widetilde{F}_{1,\beta,m}(k_x)\exp(jk_x d) \tag{28}$$

$$\widetilde{F}_{2,\alpha,n}(k_x) = \widetilde{F}_{1,\alpha,n}(k_x)\exp(jk_x d). \tag{29}$$

d being the distance between microstrips. The independent elements for the matrix equation associated with the EFIE in (22) are the same as in [8], i.e.,

$$b_{1,m}(k_z) = \delta_{\beta,z}\delta_{m,0} \tag{30}$$

where $\delta_{\beta,z}\delta_{m,0}$ are the Kronecker deltas. The independent elements for the matrix equation associated with the EFIE in (23) are given by

$$\begin{aligned}
&b_{2,m}(k_z)\\
&\quad = -\frac{1}{2\pi}\int_{C_{k_x}} dk_x \left[\widetilde{F}_{2,\beta,m}(k_x^*)\right]^*\\
&\qquad \cdot \left\{\widetilde{G}_{\beta\alpha}(k_x,k_z)\widetilde{J}_{1,\alpha}(k_x,k_z) + \widetilde{G}_{\beta\beta}(k_x,k_z)\widetilde{J}_{1,\beta}(k_x,k_z)\right\}
\end{aligned} \tag{31}$$

where $\widetilde{J}_{1,\alpha}(k_x,k_z)$ and $\widetilde{J}_{1,\beta}(k_x,k_z)$ are the two-dimensional (2-D) Fourier transform of $J_{1,x}(x,z)$ and $J_{1,z}(x,z)$ in (24). Both $\widetilde{J}_{1,\alpha}(k_x,k_z)$ and $\widetilde{J}_{1,\beta}(k_x,k_z)$ are computed by solving the matrix equation associated with the EFIE in (22) and then are introduced in (31). The Green's function in (31) has two different complex poles $k_{x,p} = \beta_x - j\alpha_x$ in the complex k_x-plane given by the two different wavenumbers of the MSSW along the x-direction [4], [8]. Since $\beta_x d \gg 1$, the integrand in (31) oscillates very fast and, therefore, the major contribution to the integral is given by the residue-pole contribution at $k_x = k_{x,p}$. Since microstrip 1 essentially radiates along the x-positive axis (assuming that the dc-bias field is directed along the z-positive axis), the pole that contributes to the integral is the pole with $\beta_x > 0$, $\alpha_x > 0$. Taking this into account, and after applying Cauchy's theorem, the integral in (31) results as follows:

$$\begin{aligned}
b_{2,m}(k_z) = j\left[\widetilde{F}_{2,\beta,m}\left(k_{x,p}^*\right)\right]^*\\
\cdot \left\{\text{Res}\left[\widetilde{G}_{\beta\alpha}(k_{x,p},k_z)\right]\widetilde{J}_{1,\alpha}(k_{x,p},k_z)\right.\\
\left. + \text{Res}\left[\widetilde{G}_{\beta\beta}(k_{x,p},k_z)\right]\widetilde{J}_{1,\beta}(k_{x,p},k_z)\right\}.
\end{aligned} \tag{32}$$

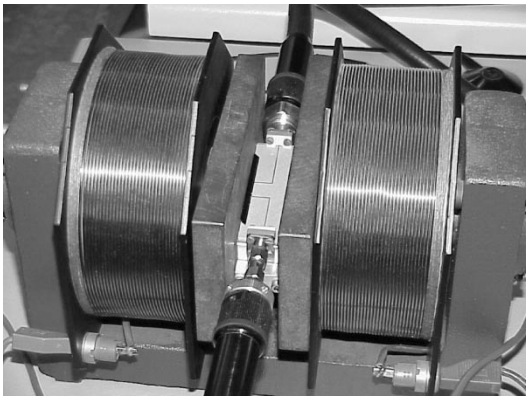

Fig. 3. Photograph of the experimental setup.

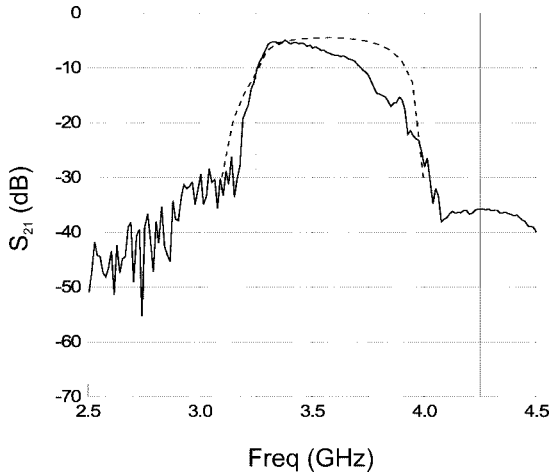

Fig. 4. Transmission response of a transducer with structural parameters, as shown in Fig. 1(a)–(c). Dielectric layer: $h_1 = 0.635$ mm, $\varepsilon_{r1} = 10$. YIG film: $h_2 = 40\ \mu$m, $\varepsilon_{r2} = 10$, width $l = 3$ mm, $4\pi \mathrm{m}_s = 1880$ G, $\Delta H = 0.6$ Oe. GGG substrate: $h_3 = 0.5$ mm, $\varepsilon_{r3} = 15$. The strip width is $w = 100\ \mu$m in the YIG-loaded section and $w = 0.605$ mm in the unloaded section. A tapered section was made between both sections. The distance between strips is $d = 10$ mm. $H_0 = 500$ Oe. Solid line: measurement. Dashed line: theory. Theoretical value of the insertion loss: 5.6 dB.

It is worth mentioning that it has been verified numerically that $\widetilde{I}_{z,0}(k_z)$ has a dependence on k_z of the kind theoretically derived in (19).

III. Results

The theoretical method presented in this paper has been checked with experiments. Fig. 3 shows a picture of the experimental setup used for the measurements. A YIG film 40-μm thick, 3-mm wide, and 5-cm long was used (the saturation magnetization was $4\pi \mathrm{M}_s = 1880$ G and the width line $\Delta H = 0.6$ Oe). To minimize the ripples in the amplitude response due to wave reflections at film edges, the YIG film ends were cut at an angle of 45° in the plane of the film. The YIG film was mounted on a printed circuit with two microstrips in the manner shown in Fig. 1(a). The required magnetic bias field in the plane of the film and perpendicular to the long axis of the YIG film [z-direction in Fig. 1(a)–(c)] was provided by an electromagnet, as shown in Fig. 3. The measurements were carried out using an HP 8510 B automatic network analyzer.

Figs. 4–6 show the measured transmission response (S_{21} in decibels) for the transducer shown in Fig. 3 when the YIG film is mounted on different dielectric substrates [the structural parameters shown in the caption of Figs. 4–6 correspond to the structural parameters depicted in Fig. 1(a)–(c)]. In all the measurements shown in these figures, the distance between strips was 1 cm [$d = 1$ cm in Fig. 1(a)–(c)], the dc-bias magnetic field was set to $H_0 = 500$ Oe and the strip width in the unloaded section of the microstrips was properly chosen in order to get a characteristic impedance of 50 Ω [$Z = 50\ \Omega$ in (5)].

Figs. 4–6 also show our results for the computation of the transmission coefficient S_{21} in decibels by using the method presented in this paper (h_i and ε_{ri} with $i = 1, 2, 3$ in the caption of these figures correspond, respectively, to the thickness and dielectric constant of the different layers of the structure). The convergence of the theoretical results was achieved by taking $N = 6$ in (24). Fig. 4 shows the measured transmission response for the transducer when the YIG film was mounted on an alumina substrate. The strip width was 100 μm in the YIG-loaded section (a tapered section was made between the YIG-loaded and unloaded sections). This figure shows that there is a good

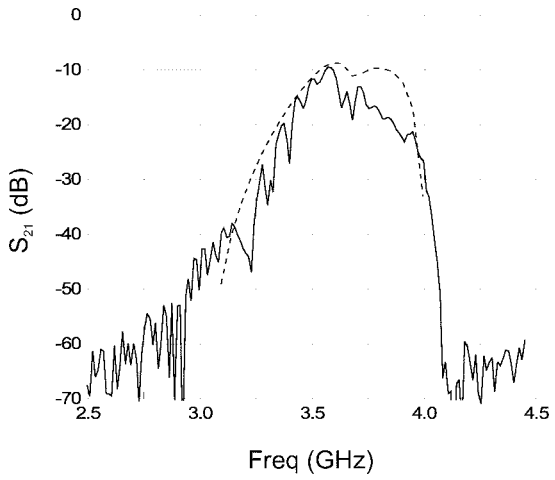

Fig. 5. Transmission response of a transducer with structural parameters, as shown in Fig. 1(a)–(c). Dielectric layer: $h_1 = 0.135$ mm, $\varepsilon_{r1} = 2.53$. YIG film: $h_2 = 40\ \mu$m, $\varepsilon_{r2} = 10$, width $l = 3$ mm, $4\pi \mathrm{m}_s = 1880$ G, $\Delta H = 0.6$ Oe. GGG substrate: $h_3 = 0.5$ mm, $\varepsilon_{r3} = 15$. The strip width is $w = 0.375$ mm in both the YIG-loaded section and the unloaded section. The distance between strips is $d = 10$ mm. $H_0 = 500$ Oe. Solid line: measurement. Dashed line: theory. Theoretical value of the insertion loss: 8.2 dB.

agreement between both theoretical and experimental results in the low-frequency region and that our method predicts the maximum value of the transmission coefficient, i.e., the insertion loss, with high accuracy. The disagreement between theory and experiment in the high-frequency region is due to the only approximation introduced in the computations. This approximation consists of the substitution of the integral in (31) by the residue-pole contribution of the integrand, as shown in (32). The integrand in (31) oscillates very fast since it contains the exponential term $\exp(jk_x d)$ (with $k_x = \beta_x - j\alpha_x$) and this introduces the functions $\cos(\beta_x d)$ and $\sin(\beta_x d)$, which are highly

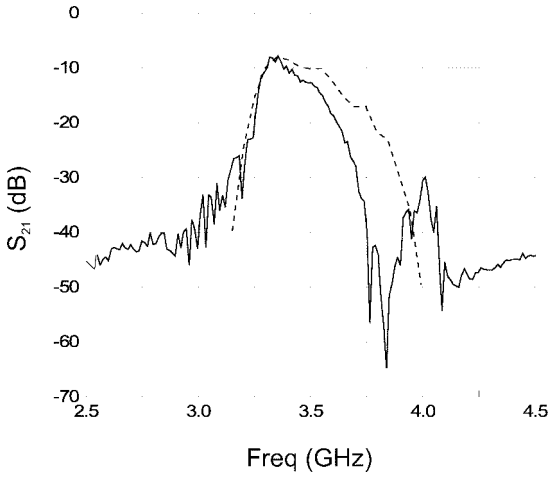

Fig. 6. Transmission response of a transducer with structural parameters, as shown in Fig. 1(a)–(c). Dielectric layer: $h_1 = 0.49$ mm, $\varepsilon_{r1} = 2.43$. YIG film: $h_2 = 40\ \mu$m, $\varepsilon_{r2} = 10$, width $l = 3$ mm, $4\pi m_s = 1880$ G, $\Delta H = 0.6$ Oe. GGG substrate: $h_3 = 0.5$ mm, $\varepsilon_{r3} = 15$. The strip width is $w = 1.43$ mm in both the YIG-loaded section and the unloaded section. The distance between strips is $d = 10$ mm. $H_0 = 500$ Oe. Solid line: measurement. Dashed line: theory. Theoretical value of the insertion loss: 8.4 dB.

oscillatory since $\beta_x d \gg 1$. The integral shown in (31) will converge very slowly and will increase the CPU time required to have accurate results. One of the purposes of the authors has been to develop a quick and accurate computational tool for the analysis of the transducers. Thus, the convergence of the integrations that provide the elements of the matrix of moments (27) has been accelerated by applying asymptotic techniques, and the convergence of the integration in (31) has been also accelerated by approximating the integral (31) by the residue-pole contribution of the integrand, as in (32). Nevertheless, this is a good approximation if the poles of the integrand in (31) are close to the real axis in the complex k_x-plane. As the frequency increases, these poles move far from the real axis and their influence on the integrand diminishes so that to approximate the integral (31) by the residue-pole contribution in this case leads to overestimate the value of the integral at high frequencies. Nevertheless, the maximum value of the transmission coefficient, i.e., the insertion loss, is very well estimated, being that this value is an essential design parameter

In Figs. 5 and 6, structures that are not usual in practical MSSW devices have been analyzed in order to investigate the possibilities of our method. Fig. 5 shows both experimental and theoretical results for the transducer when the YIG film is mounted on a low-permittivity dielectric substrate. The strip width was the same for both the YIG-loaded section and the unloaded section microstrip lines. A good agreement between both experimental and theoretical results is also shown for this case. Finally, Fig. 6 shows the results for a low-permittivity dielectric substrate and a very wide strip width (in this case, the strip width was the same for both the YIG-loaded and unloaded sections). The theoretical maximum value of the insertion loss agrees with the measured value. Since the strip width is very wide, the current distribution in this case can only be well determined by means of a full-wave analysis, as was shown in [8], where the input impedance of this same structure was measured and computed. Actually, this structure is analyzed in this paper to make clear that, in spite of a transmission-line model being used in our method, the method is not a mere quasi-TEM approach.

IV. Conclusion

A method has been presented for the computation of the transmission response of MSSW microstrip transducers. The method is based on a transmission-line model, which takes into account the nonuniform nature of both the current distribution across the strip width and the fields along the YIG film. Since the transmission-line parameters of the model are computed following a full-wave analysis and the nonuniform nature of the fields along the YIG-loaded microstrip section is included in the model, the method can be applied to the analysis of MSSW transducers with very variable geometries.

Acknowledgment

The authors wish to thank Prof. N. G. Kovshikov, St. Petersburg University, St. Petersburg, Russia, for his suggestions to this study during his visit to the Department of Electronics and Electromagnetism, University of Seville, Seville, Spain.

References

[1] A. K. Ganguly and D. C. Webb, "Microstrip excitation of magnetostatic surface waves: Theory and experiment," *IEEE Trans. Microwave Theory Tech.*, vol. MTT-23, pp. 998–1006, Dec. 1975.

[2] A. K. Ganguly, D. C. Webb, and C. Banks, "Complex radiation impedance of microstrip-excited magnetostatic-surface waves," *IEEE Trans. Microwave Theory Tech.*, vol. MTT-26, pp. 444–447, June 1978.

[3] J. C. Sethares, "Magnetostatic surface-wave transducers," *IEEE Trans. Microwave Theory Tech.*, vol. MTT-27, pp. 902–909, Nov. 1979.

[4] J.-H. Lee and J.-W. Ra, "Full-wave calculation of the radiation impedance of microstrip-excited magnetic surface waves," *Microwave Opt. Technol. Lett.*, vol. 6, no. 7, pp. 441–444, June 1993.

[5] T. W. O'Keeffe and R. W. Patterson, "Magnetostatic surface-wave propagation in finite samples," *J. Appl. Phys.*, vol. 49, no. 9, pp. 4886–4895, Sept. 1978.

[6] G. A. Vugalter and I. A. Gilinski, "Excitation and reception of magnetostatic waves by a microstrip transducer," *Sov. Phys.—Tech. Phys.*, vol. 30, no. 11, pp. 1332–1334, Nov. 1985.

[7] V. F. Dimitriev, B. A. Kalinikos, and N. G. Kovshikov, "Experimental study of the radiation impedance of microstrip spin-wave antennas," *Sov. Phys.—Tech. Phys.*, vol. 31, no. 11, pp. 1300–1305, Nov. 1986.

[8] M. J. Freire, R. Marqués, and F. Medina, "Full-wave analysis of the excitation of magnetostatic-surface waves by a semi-infinite microstrip transducer: Theory and experiment," *IEEE Trans. Microwave Theory Tech.*, vol. 51, pp. 903–907, Mar. 2003.

[9] W. S. Ishak, "Magnetostatic wave technology: A review," *Proc. IEEE*, vol. 76, pp. 171–187, Feb. 1988.

[10] P. Kabos and V. S. Stalmachov, *Magnetostatic Waves and Their Applications*. London, U.K.: Chapman & Hall, 1994.

[11] H. J. Wu, C. V. Smith, J. H. Collins, and J. M. Owens, "Bandpass filtering with multibar magnetostatic-surface wave microstrip transducers," *Electron. Lett.*, vol. 13, no. 20, pp. 610–611, Sept. 1977.

[12] H. J. Wu, C. V. Smith, and J. M. Owens, "Bandpass filtering and input impedance characterization for driven multielement transducer pair-delay line magnetostatic wave devices," *J. Appl. Phys.*, vol. 50, no. 3, pp. 2455–2457, Mar. 1979.

[13] S. N. Bajpai, R. L. Carter, and J. M. Owens, "Insertion loss of magnetostatic surface wave delay lines," *IEEE Trans. Microwave Theory Tech.*, vol. 36, pp. 132–136, Jan. 1988.

Manuel J. Freire was born in Cádiz, Spain, in 1972. He received the Licenciado and Ph.D. degrees in physics from the University of Seville, Seville, Spain, in 1995 and 2000, respectively.

From 1995 to 1996, he served in the Royal Naval Observatory, Spanish Navy, San Fernando, Cádiz, Spain. In 1996, he joined the Microwave Group, Department of Electronics and Electromagnetics, University of Seville. In 1998, he was a Visiting Researcher with the Department of Electrical and Computer Engineering, University of Houston, Houston, TX. He is currently an Assistant Professor with the Department of Electronics and Electromagnetics, University of Seville. His research interests include leakage in microstrip lines, magnetostatic-wave propagation in ferrite devices, and frequency-selective surfaces.

Dr. Freire was the recipient of a grant presented by the Spanish Ministry of Education.

Ricardo Marqués (M'95) was born in San Fernando, Cádiz, Spain. He received the Licenciado and Doctor degrees from the University of Seville, Seville, Spain, in 1983 and 1987, respectively, both in physics.

Since 1984, he has been with the Department of Electronics and Electromagnetism, University of Seville, where he is currently an Associate Professor. His main fields of interest include computer-aided design (CAD) for microwave integrated-circuit (MIC) devices, wave propagation in ferrites, and other complex anisotropic and/or bi-isotropic media and field theory.

Francisco Medina (M'90–SM'01) was born in Puerto Real, Cádiz, Spain, in November 1960. He received the Licenciado and Doctor degrees from the University of Seville, Seville, Spain, in 1983 and 1987, respectively, both in physics.

From 1986 to 1987, he spent the academic year with the Laboratoire de Microondes de l'ENSEEIHT, Toulouse, France. From 1985 to 1989, he was a Profesor Ayudante (Assistant Professor) with the Department of Electronics and Electromagnetism, University of Seville, and since 1990, he has been a Profesor Titular (Associate Professor) of electromagnetism. He is also currently Head of the Microwaves Group, University of Seville. His research interest includes analytical and numerical methods for guidance, resonant and radiating structures, passive planar circuits, and the influence on these circuits of anisotropic materials.

Dr. Medina was a member of both the Technical Program Committee (TPC) of the 23rd European Microwave Conference, Madrid, Spain, 1993, and the TPC of ISRAMT'99, Malaga, Spain. He is on the Editorial Board of the IEEE TRANSACTIONS ON MICROWAVE THEORY AND TECHNIQUES. He has been a reviewer for other IEEE and Institution of Electrical Engineers (IEE), U.K., publications. He was the recipient of a Ministerio de Educación y Ciencia/Ministere de la Recherche et la Technologie Scholarship.